Analysis of spurious events in seismic interferometry

Jan Thorbecke and Kees Wapenaar
Delft University of Technology, The Netherlands

Abstract

Seismic interferometry can be used to construct the Green's function between two buried receivers in the subsurface. To construct the exact Green function sources should be placed at a surface enclosing the buried receivers. In practice sources could only be placed at the surface, and spurious events are introduced in the constructed Green's function due to the missing sources. The origin of these spurious events are analysed and methods to reduce the amplitude of these events are investigated.

Introduction

Seismic interferometry (SI) is the process of generating new seismic reflection responses by cross-correlating observations of sources at different receiver locations. This process can be used in passive seismics where seismic events of natural sources are correlated to construct reflection data (Draganov et al. 2006). In the case of one-sided illumination with active sources (Wapenaar, 2006) SI can be used to construct the Green function between two buried receivers (also called virtual source responses by Korneev and Bakulin, 2006). The basis of all these methods is the time-correlation between two measured traces followed, by a summation of the contribution from different sources. In practice the number of sources is always limited and artefacts (Schuster et al., 2003, Snieder et al., 2006a) are introduced in the reconstructed signal. In this paper we will start by briefly mentioning the approximations introduced in SI. An artificial, but interesting, way to suppress the spurious events is shown and the influence of the in-homogeneity of the medium in the constructed Green's function is investigated.

Approximations in Seismic interferometry

Consider a Green's function $G(\mathbf{x}, \mathbf{x}_A, t)$ for an inhomogeneous lossless acoustic medium, where $\mathbf{x}$ and $\mathbf{x}_A$ are the Cartesian coordinate vectors for the observation and source points, respectively, and where t denotes time. We define the temporal Fourier transform as $\hat{G}(\mathbf{x}, \mathbf{x}_A, \omega) = \int_{-\infty}^{\infty} \exp(-j\omega t) G(\mathbf{x}, \mathbf{x}_A, t) \mathrm{d}t$, where j is the imaginary unit and ω the angular frequency. Assuming the unit point source at $\mathbf{x}_A$ is of the volume injection rate type, the wave equation for $\hat{G}(\mathbf{x}, \mathbf{x}_A, \omega)$ reads

$$\rho \partial_i (\rho^{-1} \partial_i \hat{G}(\mathbf{x}, \mathbf{x}_A, \omega)) + (\omega^2/c^2) \hat{G}(\mathbf{x}, \mathbf{x}_A, \omega) = -j\omega\rho\delta(\mathbf{x} - \mathbf{x}_A). \tag{1}$$

Here $c = c(\mathbf{x})$ and $\rho = \rho(\mathbf{x})$ are the propagation velocity and mass density of the inhomogeneous medium and ∂_i denotes the partial derivative in the x_i-direction. The representation of $\hat{G}$, as derived for seismic interferometry from Rayleigh's reciprocity theorem, reads

$$2\Re\{\hat{G}(\mathbf{x}_A, \mathbf{x}_B, \omega)\} = \oint_{\partial\mathbb{D}} \frac{-1}{j\omega\rho(\mathbf{x})} \Big(\hat{G}^*(\mathbf{x}_A, \mathbf{x}, \omega) \partial_i \hat{G}(\mathbf{x}_B, \mathbf{x}, \omega) - \big(\partial_i \hat{G}^*(\mathbf{x}_A, \mathbf{x}, \omega)\big) \hat{G}(\mathbf{x}_B, \mathbf{x}, \omega) \Big) n_i \mathrm{d}^2\mathbf{x}, \tag{2}$$

where $\partial\mathbb{D}$ is an arbitrary closed surface with outward pointing normal vector $\mathbf{n} = (n_1, n_2, n_3)$, $\Re$ denotes the real part, and the asterisk $(*)$ complex conjugation (Wapenaar et al., 2005). The points $\mathbf{x}_A$ and $\mathbf{x}_B$ are both situated inside $\partial\mathbb{D}$. Note that equation 2 is exact and applies to any lossless arbitrary inhomogeneous fluid medium. The choice of the integration boundary $\partial\mathbb{D}$ is arbitrary as long as it encloses $\mathbf{x}_A$ and $\mathbf{x}_B$, and the medium may be inhomogeneous inside as well as outside $\partial\mathbb{D}$.
For the interpretation of the seismic interferometric representation, equation 2, we refer to Figure 1a. The Green's functions under the integral are responses of monopole and dipole sources at $\mathbf{x}$ on the boundary $\partial\mathbb{D}$, observed by receivers at $\mathbf{x}_A$ and $\mathbf{x}_B$. The products $\hat{G}^* \partial_i \hat{G}$ and $(\partial_i \hat{G}^*)\hat{G}$ correspond to crosscorrelations at these observation points; the integral is taken along the sources on $\partial\mathbb{D}$. The expression in the left-hand side of equation 2 is the Fourier transform of $G(\mathbf{x}_A, \mathbf{x}_B, t) + G(\mathbf{x}_A, \mathbf{x}_B, -t)$, which is the superposition of the response at $\mathbf{x}_A$ due to an impulsive source at $\mathbf{x}_B$ and its time-reversed version. Since the Green's function $G(\mathbf{x}_A, \mathbf{x}_B, t)$ is causal, it can be obtained by taking the causal part of this superposition.
Based on equation 2 Wapenaar and Fokkema (2006) derived a mathematical expression which is directly suited for seismic interferometry in the field and is given by:

$$\Re\{\hat{G}(\mathbf{x}_A, \mathbf{x}_B, \omega)\} \approx \oint_{\partial\mathbb{D}} \frac{2}{c\rho} \hat{G}^*(\mathbf{x}_A, \mathbf{x}, \omega) \hat{G}(\mathbf{x}_B, \mathbf{x}, \omega) \mathrm{d}^2\mathbf{x}, \tag{3}$$

This equation simply states that time-correlation of measured signals, originating from (monopole) sources surrounding the measurement stations, is used to construct the Green's function between the stations by summation of contributions from different sources.
To arrive at the simple seismic interferometry equation 3 the following assumptions were made (explained in detail in Wapenaar and Fokkema, 2006):

- $\mathbb{D}$ is an inhomogeneous lossless (acoustic) medium,
- $\partial\mathbb{D}$ is an arbitrary closed surface with outward pointing normal vector $\mathbf{n} = (n_1, n_2, n_3)$ and encloses $\mathbf{x}_A$ and $\mathbf{x}_B$,
- the medium may be inhomogeneous inside $\partial\mathbb{D}$ but homogeneous outside $\partial\mathbb{D}$,
- the Fraunhofer far-field approximation is made,
- the sources are assumed to be impulsive point sources.

When one or more of these assumptions are violated, the effects on the reconstructed Green's function are:

- spurious events due to incomplete cancellation of contributions from different stationary points,
- an amplitude error.

The approximations used to derive equation 3 do not affect the phase and is therefore still very useful to construct Green's functions. However, the artificial spurious events are confusing if one wants to interpret constructed events as reflections from earth layers. In the following section two simple examples are used to illustrate the spurious events caused by an incomplete integration surface, and ways are investigated to reduce its amplitude.

Spurious events from integration surface

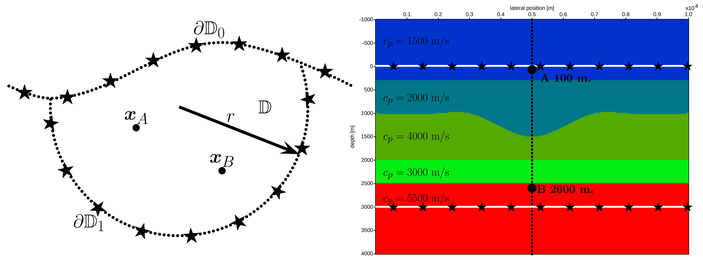

a) Integration domain for SI b) Simple model with source contributions.

FIGURE 1: *a) For Green's function retrieval between two points within the closed surface ($\boldsymbol{x}_A$ and $\boldsymbol{x}_B$), for example from buried receivers, sources are needed on both $\partial\mathbb{D}_0$ and $\partial\mathbb{D}_1$. In controlled source acquisition, $\partial\mathbb{D}_1$ does not contain sources and the effects of this missing part of the integral is investigated in this paper.*
b) At depth levels $z = 0$ and $z = 3000$ m, every 12 meter a source is placed between 0 and 10000 m. Two buried receivers are placed in the middle of the model. The top, bottom and sides of the model are absorbing the incoming energy.

Seismic interferometry equation 3 can be used to construct the Green's function between two buried receivers. As shown in Figure 1a the integral is carried out along a closed surface for a complete reconstruction of all events. Wapenaar (2006) showed that the contribution of $\partial\mathbb{D}_1$ can be neglected if the radius r becomes very large and the medium inside $\partial\mathbb{D}$ is inhomogeneous. The idea is that due to the inhomogeneities inside $\partial\mathbb{D}$ most of the energy transmitted from sources at $\partial\mathbb{D}_0$ is reflected back (multiple scattering) into $\partial\mathbb{D}$ and measured by the buried receivers.
To illustrate SI, and the construction of reflection events, a simple model with only a few layers is used and shown in Figure 1b. Two detectors are placed in the model; one just below the array of sources ($\mathbf{x}_A$) and another one below the deepest reflector ($\mathbf{x}_B$). To reconstruct the Green's function between those two detectors an array of sources at $z = 0$ and an array at $z = 3000$ m is used. Correlation panels are constructed by correlating the response of each source at $\mathbf{A}$ with the response of each source at $\mathbf{B}$. The summation over the traces in a correlation panel gives a single trace representing the Green's function between $\mathbf{x}_A$ and $\mathbf{x}_B$. This trace is shown in Figure 2a for the array of sources at $z = 0$. In the correlation panel one can clearly observe the stationary points around $x = 5000$, which contribute in the constructed (red) trace. The green trace shows the correct Green's function. Note that before the first arrival spurious events (indicated with an arrow) are present in the constructed red trace.
The spurious events in Figure 2a have their largest amplitude close to $t = 0$ and their amplitude decays strongly for increasing times. Following Snieder et al., (2006b) it is argued that spurious events have an amplitude proportional to the power of 2 of the reflection coefficient r. Figure 2b shows the constructed trace using the array of sources at $z = 3000$. The contribution from this array largely compensates the spurious events present in 2a. The summation of the result of 2a and 2b is shown in 3a. In practice one cannot place sources in depth and other ways have to be found to suppress spurious events. By correlation with the down-going wavefield at $\mathbf{A}$, Mehta et al., (2007) showed that spurious events are also suppressed. The results of this approach is shown in Figure 3e and Figure 4. In this case the position of $\mathbf{A}$ is in the same layer as the sources and the reconstructed trace with the down-going field is identical to a downward extrapolating result. In the next example we will discuss a more complicated situation.

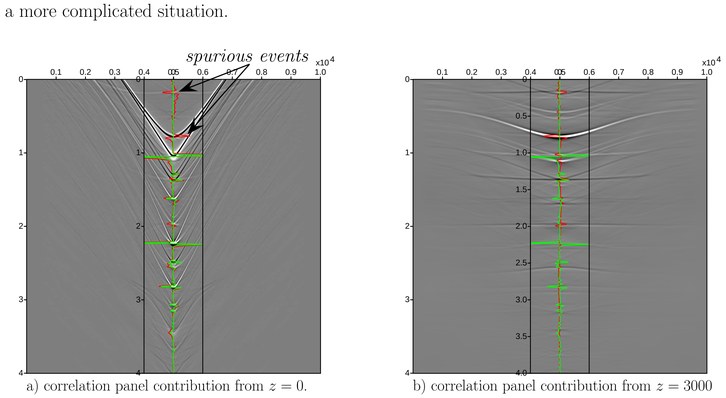

a) correlation panel contribution from $z = 0$. b) correlation panel contribution from $z = 3000$

FIGURE 2: *The correlation panel and the reconstructed trace from the source array at $z = 0$ (a). Spurious events (indicated with an arrow) are present in the reconstructed (red) trace. The green trace represents the correct Green's function. b) show the correlation panel between $\mathbf{x}_A$ and $\mathbf{x}_B$ with sources at $z = 3000$ m.*

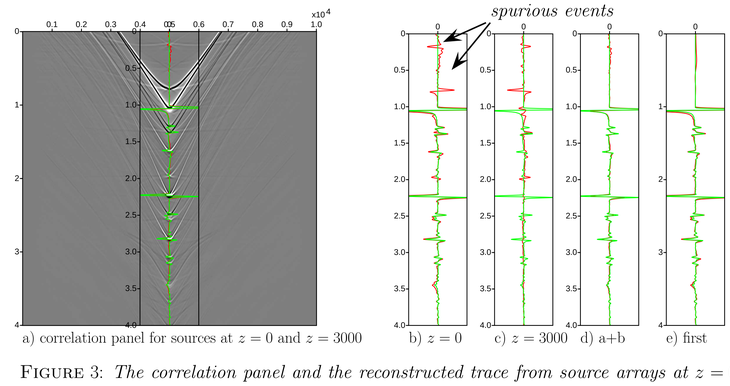

a) correlation panel for sources at $z = 0$ and $z = 3000$ b) $z = 0$ c) $z = 3000$ d) a+b e) first

FIGURE 3: *The correlation panel and the reconstructed trace from source arrays at $z = 0$ and $z = 3000$ m (a). Comparison between reconstructed Green's functions using integration surfaces at $z = 0$ (b) and $z = 3000$ m (c), both surfaces (d) and using only the first arrival in $\boldsymbol{x}_A$ (e).*

Analysis of spurious events in seismic interferometry

Jan Thorbecke and Kees Wapenaar
Delft University of Technology, The Netherlands

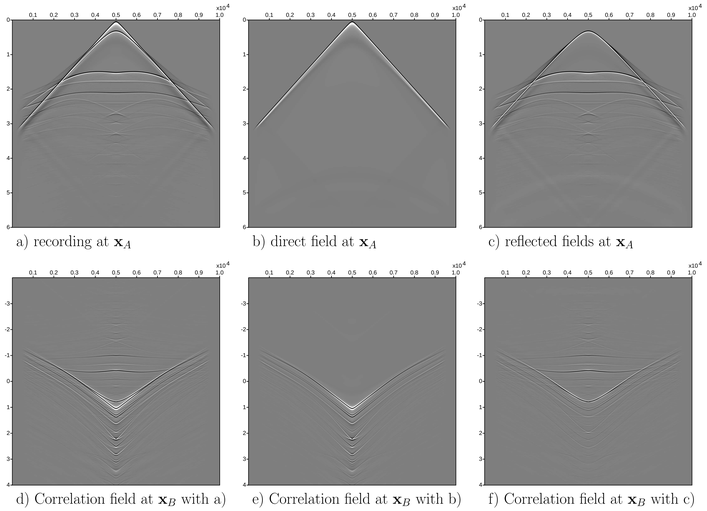

a) recording at $\mathbf{x}_A$ b) direct field at $\mathbf{x}_A$ c) reflected fields at $\mathbf{x}_A$

d) Correlation field at $\mathbf{x}_B$ with a) e) Correlation field at $\mathbf{x}_B$ with b) f) Correlation field at $\mathbf{x}_B$ with c)

FIGURE 4: *The total measured wavefield at the buried detector location $\mathbf{x}_A$ is shown in a), whereas b) shows only the direct field and c) the reflected field. The result of correlation with the measured wavefield at $\mathbf{x}_B$ is shown at d), e) and f) for respectively the total field (a), direct field (b) and reflected field (c) at $\mathbf{x}_A$.*

Figure 4 shows the correlation panels of the total, direct and reflected wavefield at $\mathbf{x}_A$ correlated with the total wavefield at $\mathbf{x}_B$. In this specific case ($\mathbf{x}_A$ is situated in the same homogeneous layer as the sources) correlation with the direct field gives an artefacts free reconstruction. Note that according to the theory the reconstructed Green's function (not the correlation panel) should be symmetric at $t = 0$.
As observed in the previous example spurious events are introduced in the constructed Green's function because the closed integral is only represented by sources at $z = 0$ m. Following the arguments of Wapenaar (2006) these spurious events should disappear when all down-going energy is reflected back to the surface. In the simple model we can achieve this by turning on completely reflecting boundaries in the finite-difference modeling code. Although this is not realistic, this simple modeling exercise shows the principle well. In the next example we will consider a more realistic situation.

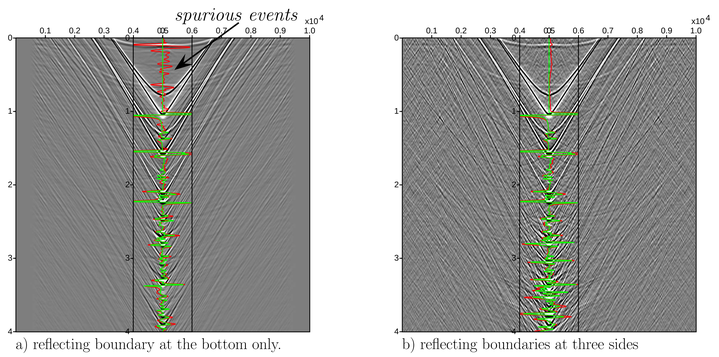

a) reflecting boundary at the bottom only. b) reflecting boundaries at three sides

FIGURE 5: *a) At the bottom of the model a completely reflecting boundary was placed and the correlation panel and trace were constructed. The spurious events (indicated with an arrow) are still present in the constructed (red) trace). The green trace represents the correct Green's function.*
b) At the bottom, left and right sides of the model completely reflecting boundaries are used and a correlation-trace and panel were constructed. The spurious events are not present anymore in the constructed (red) trace.

Figure 5a shows the correlation panel and the constructed trace when the bottom boundary of the model is completely reflecting. Note that the exact Green's function (green trace) is also changed. The red trace shows the constructed signal which still contains spurious events, clearly observed before the first arrival. In Figure 5b the left and right boundaries of the model are also made completely reflecting. In this case the reconstructed Green's functions (red trace) matches very well with the exact Green's functions and the spurious events have disappeared. Note that the stationary points which cancel the spurious events are not easy to recognise in Figure 5b.
In a strongly inhomogeneous medium, e.g. a medium with many layers, most of the energy will be reflected back to the surface and measured by the buried receivers. In a similar way, with the totally reflecting boundaries in the previous example, we expect that the constructed Green's function will be more accurate when more reflecting layers are present. To get an idea how inhomogeneous the medium must be for accurate construction of the Green's function, the model in Figure 6 with a varying number of layers, is used. The model consists of flat thin layers where each layer has a smoothly laterally varying propagation velocity (Figure 6 shows only the first 30 layers). As in the previous example two buried receivers are placed within the model and only sources at depth $z = 0$ m. are used.

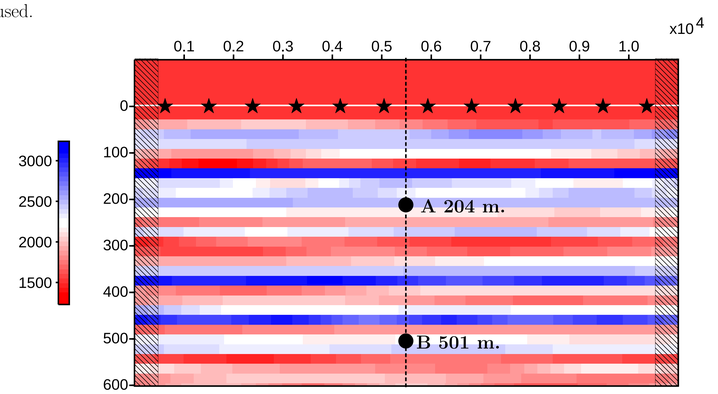

FIGURE 6: *Each layer in the model shown is 20 m thick and has a propagation velocity in the range 1300-3200 m/s. Within each layer the velocity changes laterally with 400 m/s around a central velocity between 1500 and 3000 m/s. To suppress the effects of the edges of the model the fields (p, v_x, v_z), calculated by the finite difference code, are surrounded by a large homogeneous layers and tapered with 198 points (594 m) on all sides. The tapered area is indicated with slanted lines. The peak frequency of the used Ricker wavelet is 22 Hz.*

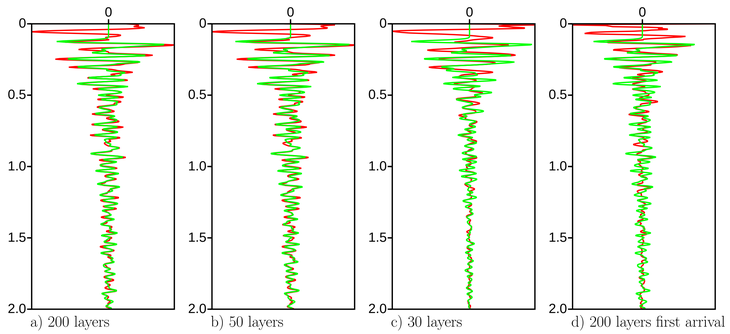

a) 200 layers b) 50 layers c) 30 layers d) 200 layers first arrival

FIGURE 7: *SI constructed traces from buried detectors in the laterally variant model shown in Figure 6 with 200 layers (only the first 30 layers are shown in Figure 6). The number of thin layers in the model is different for the results shown in a,b and c. The complete wavefields at position* **A** *and* **B** *are used. For the reflecting part there is no significant difference between the Green's function (green line) and the constructed trace (red line) in a model with 200 (a) and 50 (b) layers. For 30 (c) layers differences are becoming visible.*

Note that the Green's function has also changed. The reconstructed trace shown in (d) in constructed by using a first arrival (obtained by time windowing) at position **A**. *In this case the reconstructed trace is different from the actual Green's function.*

The constructed Green's functions, with different numbers of layers in the propagation model, are shown in Figure 7a, b and c. It is surprising to see that even in a model with only 50 (Figure 7b) layers the reconstruction is still acceptable. Before the first arrival strong spurious events are observed in all constructed traces. These events originate from 'leakage' to the sides of the model. They will disappear if additional sources at the sides are used (and close the integration surface) or if the medium is stronger inhomogeneous in lateral sense.
Figure 7d shows in red the reconstructed trace when only the first arrival of the wavefield at **A** is used. The first arrival was obtained by time windowing the total recording at **A**. The reconstructed trace (red line) contains some of the main events, but also contains spurious events. The complexity of the medium makes this approach less successful as the 4 layer example of Figure 1b. For a better reconstruction not only the first arrival at **A** should be used, but the complete downgoing wavefield. Another way to reduce the amplitude of the spurious events is to use deconvolution instead of correlation (Snieder et al., 2006a; Wapenaar et al., 2008). The deconvolution approach is currently investigated in our group at the University of Delft.

Conclusions

Seismic interferometry can be used to construct the Green's function between two buried receivers using only sources at the surface. From the theory it follows that a closed surface integral, of source positions surrounding the buried receivers, is required. Replacing the closed surface by an open surface (at which the sources are located) introduces artefacts. There are two complementary ways of suppressing these artefacts. In mildly inhomogeneous media it is sufficient to select the first arrival of the wave field at A and correlate it with the field at B. The accuracy of this approach decreases with increasing complexity of the medium. On the other hand, we can correlate the total fields at A and B, relying on the assumption that the downgoing energy is reflected back by the inhomogeneities of the medium. The accuracy of this second approach increases with increasing complexity of the medium.

Acknowledgements

The authors wish to thank StatoilHydro for their financial support of this research.

References

Draganov, D., C. Wapenaar, and J. Thorbecke, 2006, Seismic interferometry: Reconstructing the earth's reflection response: Geophysics, **71**, SI61–SI70.
Korneev, V. and A. Bakulin, 2006, On the fundamentals of the virtual source method: Geophysics, **73**, A13–A17.
Mehta, K., A. Bakulin, J. Sheiman, R. Calvert, and R. Snieder, 2007, Improving the virtual source method by wavefield separation: Geophysics, **72**, V79–V86.
Schuster, G. T., F. Followill, L. J. Katz, J. Yu, and Z. Liu, 2003, Autocorrelogram migration: Theory: Geophysics, **68**, 1685–1694.
Snieder, R., J. Sheiman, and R. Calvert, 2006a, Equivalence of the virtual-source method and wavefield deconvolution in seismic interferometry: Physical Review E., **73**, 1–9.
Snieder, R., K. Wapenaar, and K. Larner, 2006b, Spurious multiples in seismic interferometry of primaries: Geophysics, **71**, SI111–SI124.
Wapenaar, K., 2006, Green's function retrieval by cross-correlation in case of one-sided illumination: Geophysical Research Letters, **33**, 1–6.
Wapenaar, K. and J. Fokkema, 2006, Green's function representations for seismic interferometry: Geophysics, **71**, SI33–SI46.
Wapenaar, K. and J. Fokkema, and R. Snieder 2005, Retrieving the Green's function in an open system by cross correlation: A comparison of approaches (L): J. Acoustical Society of America, **118**, 2783–2786.
Wapenaar, K., E. Slob, and R. Snieder, 2008, Seismic and electromagnetic controlled-source interferometry in dissipative media: Geophysical Prospecting, **56**, in press.